

Inelastic scattering of light in the antiferromagnet EuTe

S. O. Demokritov, N. M. Kreines, and V. I. Kudinov

Institute of Physics Problems, USSR Academy of Sciences

(Submitted 22 July 1986)

Zh. Eksp. Teor. Fiz. **92**, 689–703 (February 1987)

One-magnon inelastic scattering of light in the antiferromagnet EuTe by thermal magnons belonging to both branches of the excitation spectrum is studied. The dependences of the magnon frequency and of the intensity of the scattered light on the magnetic field are measured in the entire region of existence of the antiferromagnetic phase at $T = 2$ K. The contribution of the intensity of one-magnon light scattering from the exchange mechanism, which is of decisive importance for strongly canted magnetic sublattices, is separated.

1. INTRODUCTION

Brillouin scattering (BS) of light by magnons is one of the few methods that permit direct study of excitation in magnets. An investigation of BS yields information on the magnon frequency, on its dependence on the magnitude and direction of the magnon wave number \mathbf{q} , on the external magnetic field \mathbf{H} , etc. (see Ref. 1). A productive application of this method, however, is usually limited by the extremely low intensity of inelastically scattered light. A typical value of the extinction coefficient is $\sim 10^{-8}$ – 10^{-11} cm^{-1} . Besides the small relative frequency shift ($\Delta\nu/\nu \sim 10^{-5}$), this circumstance makes observation of BS by magnons a very complicated experimental task. Much attention is therefore paid in the study of BS to theoretical and experimental investigations of various scattering mechanisms.^{2–4}

The intensity of BS by magnons is known to be directly connected with the magnitudes of the magneto-optic effects (MOE) present in the crystal. Scattering mechanisms can therefore be classified in accordance with MOE that are connected with various microscopic interaction mechanisms between a light wave and magnetic system.

Brillouin scattering has by now been used to study the spin-wave spectra in certain ferro-, ferri-, and antiferromagnets.¹ Contributions of MOE that result from the presence of a large spin-orbit interaction in a magnet and are therefore of relativistic origin (the Faraday effect (FE), magnetic birefringence, circular and linear dichroism). A new single-magnon scattering of exchange origin was recently observed.⁵ The MOE corresponding to it—isotropic magnetic refraction (IMR)—describes the dependence of the refractive index on the crystal magnetization.

We use here the method of BS by thermal magnons to investigate the excitation spectra of both branches in the easy-plane antiferromagnet EuTe at $T \approx 2$ K. The dependence of the magnon frequency on the external magnetic field is obtained in a field interval 0–80 kOe that includes the entire region in which the antiferromagnetic phase exists. Investigation of the dependence of the magnon frequency on the direction of the wave vector \mathbf{q} has made it possible to separate the contribution made to the excitation spectrum by the magnetodipole interaction. A strong relaxation of one of the modes is observed when the spin-flip transition is approached. We have also investigated the intensity of BS by thermal magnons as a function of the external magnetic

field. We succeeded in separating the contributions of the principal MOE that determine the extent of the light scattering, and obtained good quantitative agreement between the experimental data and the calculated extinction coefficient. Raman scattering of light (RS) by individual Eu^{2+} ions was recorded in the paramagnetic phase ($T = 300$ K).

2. THE SAMPLES

The EuTe crystal is one of the europium chalcogenides that have a cubic structure of NaCl type (space group O_h^2). The magnetic properties of these compounds are governed by the strongly localized moment of the rare-earth ion Eu^{2+} , which has a spin $S = 7/2$ and an orbital momentum $L = 0$. The magnetic properties and magnetic structure of EuTe have by now been sufficiently well investigated. It has been shown that below $T_N = 9.8$ K it is an antiferromagnet (AF) with magnetic anisotropy of the easy plane type.^{6,7} The spins are ferromagnetically ordered in the (111) plane and their directions in the two neighboring are reversed. The effective anisotropy field H_A is ~ 10 kOe. In the antiferromagnetic state, EuTe breaks up into four AF domains (T -domains) corresponding to four equivalent (111) planes. It is impossible to bring the crystal to a single-domain state by an external magnetic field.⁸

The weak anisotropy in the (111) plane (effective field $H_a \sim 10$ Oe) leads to formation of six S -domains oriented along axes of type $[11\bar{2}]$. This domain structure vanishes in a field $H > (2H_a H_E)^{1/2}$ (spin-flop transition).⁷ The effective exchange field H_E is 36 kOe. The EuTe is transformed in an external magnetic field from the AF state into the state of a saturated paramagnet (spin-flip transition).⁹ The saturation magnetization reaches then 0.92 kG.

Antiferromagnetic resonance (AFMR) in EuTe was investigated in detail both by ordinary microwave methods^{8,10} and by using light scattering.¹¹ It was found that as the spin-flip transition is approached the frequency of one of the AFMR spectrum branches is greatly lowered.¹²

At the light wavelength ($\lambda = 632.8$ nm) used by us, EuTe crystals in a magnetically ordered state exhibit, besides a relative transparency (penetration depth 0.3 mm), strong magneto-optic effects. Thus, according to Refs. 11–13, the FE reaches at saturation $\sim 2 \cdot 10^5$ deg/cm ($n_+ - n_- = 0.07$), and the isotropic magnetic refraction is $n = 0.005$. The actual linear magnetic birefringence (LMB) is smaller by two orders. The presence of large MOE along-

side relatively small absorption is attributed to the fact that the energy of a $\lambda = 632.8$ nm photon is close to the fundamental absorption edge $E_g = 2.05$ eV due to $4f \rightarrow 5d_{2g}$ electro-dipole transitions. The spin-orbit and d - f exchange interactions split the $5d_{2g}$ level.^{14,15} Spectroscopic data yield for EuTe values of the same order (~ 0.3 eV) for this interaction. This substance is therefore subject to the different large microscopic MOE described above (FE,IMR).

Crystalline EuTe is a semiconductor. The carrier impurity density in our samples was quite low, however, and the impurities exerted no noticeable influence whatever on the initial antiferromagnetic structure.

The samples were prepared in the form of plates, with naturally cleaved two surfaces (parallel to (001)) and one end face. The plates were relatively thin ($4 \times 4 \times 1$ mm). This shape made it possible to identify with sufficient accuracy the produced demagnetizing fields. We used in our experiments EuTe crystals grown by L. A. Klinkova in the Institute of Solid State Physics of the USSR Academy of Sciences.

3. MEASUREMENT PROCEDURE. EXPERIMENTAL SETUP

We investigated in the experiment BS under backscattering (180°) conditions, i.e., with the wave vectors of the investigated magnon \mathbf{q} of the incident and reflected light \mathbf{k}_1 and \mathbf{k}_2 parallel to one another. The value of q at $\lambda = 632.8$ nm was $3 \cdot 10^5$ cm⁻¹. We used two experimental geometries, with the magnon wave vector \mathbf{q} parallel and perpendicular to the magnetization.

The principal part of the experimental setup was an optical system comprising a high-contrast high-resolution spectrometer. The setup construction is described in detail in Ref. 11; we therefore describe its operation only in general outline, without going into details.

The light source was a helium-neon laser of wavelength $\lambda = 632.8$ nm. The spectral instrument was a scanning multipass Fabry-Perot interferometer manufactured by Burleigh, with a contrast exceeding 10^8 . A DAS-1 system was used to record and accumulate the data, and also for scanning and active stabilization of the interferometer. It consisted of a multichannel analyzer and a microprocessor to control the interferometer. The scanning period was ~ 1 s, and the entire accumulation of one spectrum took 20–30 min. After the end of the accumulation, the content of the memory of the multichannel analyzer was transferred to the computer data bank. Next, after reduction, the spectrum could be extracted to a plotter when necessary. Figure 1 shows a typical plot of the scattering spectrum of EuTe at a fixed magnetic field $H = 25$ kOe and at $T = 2$ K. The intense peak with zero frequency shift (fundamental line) is due to elastic scattering of the light by the crystal defect. The shifted satellites correspond to elastic scattering of the light by the magnons. Spectra of this form permit a rather exact measurement (1%) of the frequency of the magnons participating in the scattering, and the intensity ratio of Stokes and anti-Stokes satellites. The insufficient long-time stability of the complicated optical system, however, hindered a sufficiently accurate (better than $\pm 50\%$) measurement of the field dependence of the scattering intensity. To be able to compare results of different experiments at different magnetic-field values, we changed over to relative-intensity measurements. The reference was the anomalously high intensity¹⁶ of scat-

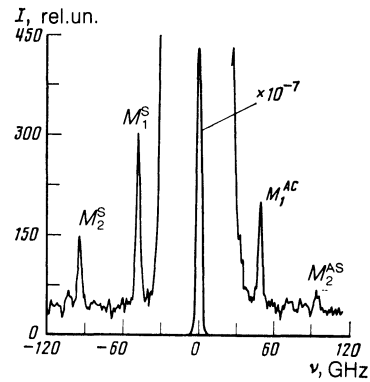


FIG. 1. Spectrum of light scattered in $T = 2$ K, $q \parallel [010] \perp \mathbf{M}$, $H = 25$ kOe.

tering by longitudinal phonons propagating along the C_4 axis in a TeO_2 crystal. We observed in one experiment simultaneously scattering both by magnons in EuTe and by phonons in TeO_2 this was effected in the following manner: A TeO_2 crystal was glued to the surface of the investigated EuTe, as shown in the inset of Fig. 2. The optical system was fitted to the common surface of the EuTe and TeO_2 . The sharpness was sufficient to be able to observe in the spectrum of the analyzed scattered light satellites corresponding to BS in both samples. Typical plots of such a spectrum are shown in Fig. 2. We measured the intensity ratio of these satellites, obtained in one and the same scattering spectrum. We used this method to study the intensity of the BS by magnons in EuTe as a function of the magnetic field (it was assumed that the intensity of BS by phonons is independent of the field). The measurement accuracy could be raised to $\pm 5\%$. These investigations were made only in the first geometry, with the wave vector of the magnon (and of the phonon in TeO_2) parallel to the external field, meaning also to the magnetization in the EuTe.

All the measurements were made at a temperature ≈ 2 K, using an optical helium cryostat with a sectionalized horizontal solenoid. The cryostat could be operated in superfluid ^4He . The maximum magnetic field produced by the solenoid was 81 kOe and was measured with a low-temperature Hall pickup. The field H was applied in the experiment along the $[001]$ axis of the EuTe crystal. At this direction,

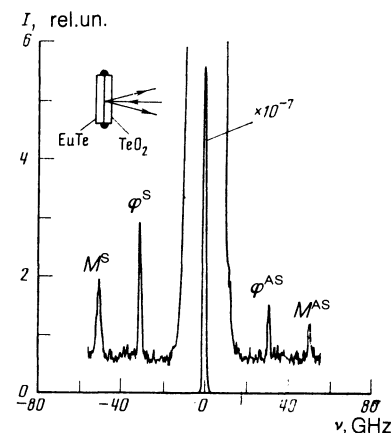


FIG. 2. Spectrum of light scattered in EuTe and TeO_2 : $T = 2$ K, $q \parallel [001] \parallel \mathbf{M}$, $H = 45$ kOe.

all the T -domains in the sample were in equivalent positions relative to the field. The energies of magnons of given \mathbf{q} , which depended on the angle between \mathbf{H} and the easy axis, were therefore the same in the different domains, and one series of satellites was observed in the scattering spectrum. Deviation of the magnetic field by more than 1° from the [001] direction would lead to a smearing of peaks in the BS spectrum. The orientation error therefore did not exceed 1° . The necessary adjustment was made by reflection of a laser beam from the cleaved surface of the sample.

In the study of the RSL at room temperature, the external magnetic field was produced by a permanent magnet and was measured by replacing the end pieces of this magnet.

4. EXPERIMENTAL RESULTS

The measurements were performed on two EuTe samples synthesized in different melts. Similar results were obtained with both samples. More experiments were performed with the sample having a deeper light penetration (~ 3 mm) and accordingly a higher scattering intensity. We cite below mainly the results obtained with this sample.

Figure 1 shows a typical scattering spectrum. It can be seen that we have succeeded in recording BS from magnons belonging to both branch of the spin-wave spectrum of an easy-plane AF. The satellites labeled M_1^S and M_1^{AS} on the spectrum correspond to scattering by magnons of the low-frequency branch of the spectrum (frequency shift $\nu_1 = 50$ GHz), and those labeled M_2^S and M_2^{AS} correspond to the high-frequency branch ($\nu_2 = 94$ GHz). Thus, one such spectrum yielded the magnon frequencies of two branches for a given magnetic field and a given direction of the wave vector \mathbf{q} relative to the crystal magnetization vector. Figure 3 shows the field dependences of the magnon frequencies of both branches for $\mathbf{q} \parallel \mathbf{M}$ and $\mathbf{q} \perp \mathbf{M}$. The abscissas of Fig. 3 (as well as of Figs. 5–7 and 9) are the values of the crystal internal magnetic field, which differs from the external one by the value of the demagnetizing field. We determined the demagnetizing coefficients assuming that a thin plate ($4 \times 4 \times 1$ mm) is close in shape to an ellipsoid having the same dimensions. The obtained demagnetizing coefficient is 0.7 in the

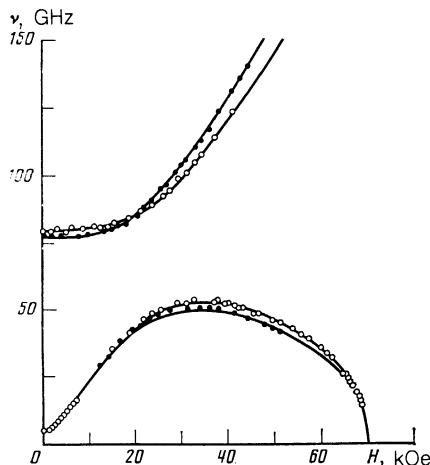


FIG. 3. Spin-wave spectrum in EuTe for $\mathbf{H} \parallel [001]$: \circ — $\mathbf{q} \parallel \mathbf{M}$, \bullet — $\mathbf{q} \perp \mathbf{M}$. Solid lines—results of theoretical calculation.

direction perpendicular to the plate plane and 0.15 along the plane. The measurement conditions were such that in a strong magnetic field ($H > 50$ kOe) it was possible to implement only the first scattering geometry ($\mathbf{q} \parallel \mathbf{M}$). The experiments have shown that at $\mathbf{q} \parallel \mathbf{M}$ the scattering intensity on the upper branch of the magnons decreases abruptly with increase of the magnetic field. As the spin-flip transition point was approached, BS was therefore observed only from the magnons of the low-frequency branch. In fields $H > 50$ kOe, however, this branch is of greater interest, since it is the soft mode of the spin-flip transition. In fact, a strong relaxation of this magnon branch was observed in experiment. In a zero magnetic field, both spectrum branches have gaps. The gap $\Delta_1 = \gamma(2H_a H_E)^{1/2}$ in the low-frequency branch is due to the pressure of intraplanar anisotropy¹⁾ H_a , and in the high frequency branch $\Delta_2 = \gamma(2H_A H_E)^{1/2}$ —to the presence of easy-plane anisotropy H_A . As seen from Fig. 3, the frequencies of the magnons propagating along the field differ from those of the magnons propagating in the perpendicular direction.

Attention is called to the difference between the intensities of the Stokes and anti-Stokes satellites on the spectrogram of Fig. 1. This difference is due to the different probability of the processes of absorption and emission of a magnon by a photon when the scattering conditions are such that $h\nu_{\text{magn}} \sim kT$. It is due to the statistics of the magnons, which are Bose particles. The ratio of the intensities of the M^S and M^{AS} satellites can be easily shown to be

$$I_S/I_{AS} = (n_\nu + 1)/n_\nu = \exp(h\nu/kT), \quad (1)$$

where $n_\nu = [\exp(h\nu/kT) - 1]^{-1}$ is a Bose distribution function proportional to the number of thermal magnons of frequency ν at a given T . It can be seen from Eq. (1) that the ratio I_S/I_{AS} for the second branch should be larger than for the first, since $\nu_2 > \nu_1$. With change of the external field, and hence of the magnon frequency, the ratio I_S/I_{AS} changes. Using Eq. (1) we can determine the temperature of the investigated volume of the sample. The obtained value ($T = 2.5$ to 3 K) shows the extent to which the investigated volume is superheated relative to the helium bath. This superheat is due to absorption of radiation power (~ 40 mW) in a light filament measuring $0.1 \times 0.1 \times 0.5$ mm.

Figure 4 shows a typical plot of the spectrum of Raman scattering of light (RSL) in paramagnetic EuTe at $T = 300$ K. In this spectrogram the Stokes and anti-Stokes satellites have the same intensity, as follows from the equal populations of the paramagnetic levels at $kT \gg h\nu$. The RSL experiments have shown that the scattering is accompanied by 90° rotation of the polarization plane. The obtained field dependence $\nu(H)$ is described by the simple law

$$\nu = \frac{1}{2\pi} g\mu_B H, \quad (2)$$

where μ_B is the Bohr magneton, and $g = 2.0$ corresponds to the pure spin magnetic moment.

The measured field dependence of the intensity of BS by magnons of the low-frequency branch at $\mathbf{q} \parallel \mathbf{M}$ is shown in Fig. 5. It can be seen that the scattering intensity is large in weak fields, decreases rapidly with increase of the field, and begins to increase again only at $H > 10$ kOe. This $I(H)$ dependence agrees with the calculation given in Sec. 6 and will be discussed in the last section of the article.

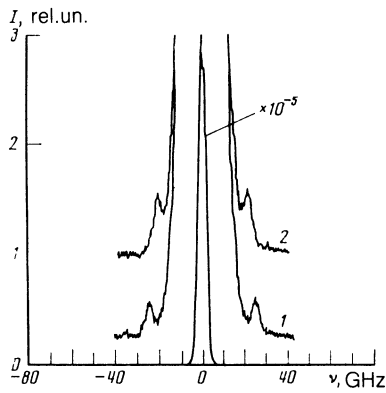


FIG. 4. Raman scattering spectrum in EuTe: $T = 300$ K, 1— $H = 8.8$ kOe, 2— $H = 7.5$ kOe.

5. ANALYSIS OF THE OBTAINED MAGNON SPECTRUM

We turn now to an analysis of the $\nu(H)$ dependence. We estimate first the contribution of the dispersion term to the magnon frequency. For magnons with a Brillouin wave vector $qB \sim 10^8 \text{ cm}^{-1}$ this contribution is $\nu \sim kT_N/h \sim 200$ GHz. For the magnons with $q \sim 10^5 \text{ cm}^{-1}$ that participate in the scattering, this contribution is much smaller ($\nu < 0.2$ GHz). The experimental error of the magnon frequency is 0.3 GHz. In our calculation of the magnon spectrum there is therefore no need to allow for the dispersion. It is impossible, however, simply to use the results of Ref. 11, where the spectrum of the AFMR (of magnons with $q = 0$) was calculated. The reason is that, as shown by experiment, the magnetodipole interaction makes under our conditions a substantial contribution to $\nu(H)$. A suitable calculation that takes this circumstance into account is based, as in Ref. 11, on the macroscopic Landau-Lifshitz equations. The calculated $\nu(H)$ for both branches in the cases $\mathbf{q} \parallel [001] \parallel \mathbf{M}$ and $\mathbf{q} \parallel [010] \perp \mathbf{M}$ are shown by the solid lines in Fig. 3. The constant H_E that enters in the calculated $\nu(H)$ dependence was taken from Ref. 9, while the values of the effective anisotropy fields H_A and H_a were determined by a best fit of the experimental points for both magnon branches to the calculation result. The values obtained were $H_A = 10.2 \pm 0.2$ kOe and $H_a = 15 \pm 1$ Oe. It should be noted that the value of H_A determined in the same manner for the second investi-

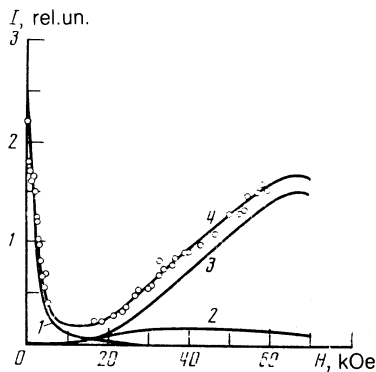


FIG. 5. Field dependence of intensity of BS by magnons of the low-frequency branch of EuTe in geometry 1. Points—experimental results, curves 1,2,3,—respective results of calculation of the contributions of the linear magnetic birefringence, of the Faraday effect, and of isotropic magnetic refraction, 4—net result.

gated sample is somewhat different ($H_A = 8.8 \pm 0.2$ kOe). Disparities in the anisotropy constants of different samples were also noted earlier.¹⁰

It is noteworthy that the $\nu(H)$ curves for the upper-branch magnons, which correspond to the cases $\mathbf{q} \parallel [001] \parallel \mathbf{M}$ and $\mathbf{q} \parallel [010] \perp \mathbf{M}$, cross. This is due to the change of the symmetry of the oscillations of the vectors \mathbf{M} and \mathbf{L} . It is known¹⁷ that the magnetodipole contribution to the magnon frequency depends substantially on the angle between the ac component of the magnetizations \mathbf{m} and \mathbf{q} . It is the variation of this angle with the field that leads to the crossing of the $\nu(H)$ curves for $\mathbf{q} \parallel \mathbf{M}$ and $\mathbf{q} \perp \mathbf{M}$.

6. CALCULATION OF THE INTENSITY OF INELASTIC LIGHT SCATTERING BY MAGNONS

To analyze the experimental results, we calculated the intensity of one magnon scattering of light for an easy-plane antiferromagnet. The calculations were based on the Landau-Lifshitz macroscopic equations for the precession of the magnetic moments, in analogy with Ref. 18., for the case when the magnetic field has arbitrary magnitude and direction.

We introduce the extinction coefficient defined as the ratio of the total intensity of the light scattered into a solid-angle element $d\Omega$ in a unit volume of the medium, in a frequency interval $d\Omega$, to the incident-light flux density. According to Ref. 19, the differential extinction coefficient in the long-wave limit is given by

$$\frac{dh}{d\Omega d\omega} = \frac{\omega^4}{32\pi^3 c^4} \int_{-\infty}^{+\infty} \langle \Delta \varepsilon_{ij}(0) \Delta \varepsilon_{ij}(t) \rangle e^{i\omega t} dt; \quad (3)$$

where ω and ω' are the frequencies of the incident and scattered light, and $\Omega = 2\pi\nu = \omega' - \omega$. The subscripts i and j specify the polarizations of the incident and scattered light, and ε_{ij} is the dielectric tensor. We express the magnetic part of the tensor ε in the form

$$\Delta \varepsilon_{ij}(\mathbf{M}, \mathbf{L}) = i f_{ijk} M_k + g_{ijkn} L_n L_n + a \delta_{ij} M^2, \quad (4)$$

where the first term describes the Faraday effect and the magnetic circular dichroism, the second the birefringence along the vector \mathbf{L} , and the third the isotropic magnetic refraction. The fluctuations of the dielectric constant, which lead to the scattering of the light, are connected by Eq. (4) with the fluctuations of \mathbf{L} and \mathbf{M} . Let $\mathbf{M}(t) = \mathbf{M}_{st} + \mathbf{m}(t)$, $\mathbf{L}(t) = \mathbf{L}_{st} + \mathbf{l}(t)$. The expansion of the tensor $\Delta \varepsilon_{ij}(t)$ in powers of small deviations of \mathbf{m} and \mathbf{l} yields then

$$\Delta \varepsilon_{ij}(t) = \Delta \varepsilon_{ij}(\mathbf{M}_{st}, \mathbf{L}_{st}) + \delta \varepsilon_{ij}(\mathbf{M}_{st}, \mathbf{L}_{st}, \mathbf{m}(t), \mathbf{l}(t)). \quad (5)$$

According to (3), the scattered-light intensity is proportional to the correlator of the dielectric tensor fluctuations $\langle \delta \varepsilon_{ij}^2 \rangle_{\Omega}$ or, with allowance for (4) and

$$I_{sc} \propto \langle \delta \varepsilon_{ij}^2 \rangle_{\Omega} \propto \langle x_k x_n \rangle_{\Omega}, \quad (6)$$

where $\mathbf{x} = (m_x, m_y, m_z, l_x, l_y, l_z)$. In analogy with Ref. 11, we use a coordinate frame with z' axis along the magnetic field \mathbf{H} and with y' axis in the easy plane ($\mathbf{L} \parallel y'$).

The correlation function $\langle x_k x_n \rangle_{\Omega}$ which determines the light scattering is known²⁰ to be connected, in accordance with the fluctuation-dissipation theorem, with the generalized susceptibility by the relation

$$\langle x_h x_n \rangle_a = -i\hbar(1+N(\Omega))[\chi_{hn}(\Omega) - \chi_{nh}^*(\Omega)], \quad (7)$$

where $N(\Omega) = [\exp(\hbar\Omega/kT) - 1]^{-1}$. The intensity of one-magnon scattering of light is thus determined by the generalized susceptibility tensor (calculated for EuTe in Ref. 11).

Each term in (4) leads, generally speaking, to light scattering. To keep the calculation simple, we consider separately the contribution of each term of (4) to the light-scattering intensity.

A. Brillouin scattering due to the Faraday effect and to circular dichroism

In crystals with cubic symmetry²⁾ the magneto-optic effects linear in \mathbf{M} are described by the following term of the dielectric tensor:

$$\Delta\epsilon_{ij}(\mathbf{M}) = i f e_{ijk} M_k, \quad (8)$$

where e_{ijk} is a unit antisymmetric tensor; $f = f' + if''$ (f' is a constant that characterizes the FE and f'' characterizes the circular dichroism). If n_0 is the refractive index of the light in the crystal, we have

$$\Phi_{FE} = \frac{\pi M_0 f'}{\lambda n_0} [\text{rad/cm}],$$

$$\Phi_{mcd} = \frac{4\pi M_0 f''}{\lambda n_0} [1/\text{cm}].$$

Let us find the alternating part of the tensor $\Delta\epsilon_{ij}(\mathbf{M})$. From (4) and (5) we obtain

$$\delta\epsilon_{ij}(t) = i f e_{ijk} m_k(t), \quad (9)$$

whence, according to (3) and (6), we can find the intensity of 180° scattering for light propagating, say, along z' :

$$\frac{dh}{d\Omega do} = \frac{\omega^4 |f|^2}{32\pi^3 c^4} \langle m_x^2 \rangle_\Omega, \quad (10)$$

with (7) taken into account, Eq. (10) becomes

$$\frac{dh}{d\Omega do} = \frac{\hbar \omega^4}{16\pi^3 c^4} |f|^2 \text{Im}(\chi_{33}(\Omega)) (1+N(\Omega)). \quad (11)$$

Similar equations can be written also for other directions of the light propagation in the crystal. It follows from (9) that in the case of MOE that are linear in \mathbf{M} the scattering is accompanied by a 90° rotation of the plane of polarization ($\delta\epsilon_{ij} = 0$ if $i = j$). Figure 6 shows the field dependence, calculated for EuTe, of the extinction coefficient, integrated over frequency, for both branches of the magnon spectrum. Here $z' \parallel \mathbf{H} \parallel [001]$. Note that the BS connected with the FE in an antiferromagnet can be different from zero at $\mathbf{k}_{\text{opt}} \parallel \mathbf{M}_{\text{st}}$. This is due to the presence of longitudinal oscillations of the magnetization in the antiferromagnet.

B. Brillouin scattering due to linear magnetic birefringence (LMB)

The second term in (4) shows that a contribution to the BR can be made by fluctuations of the AF vector \mathbf{L} . We introduce a coordinate frame x, y, z connected with the plane (111), with $z \parallel [111]$ and $y \parallel \mathbf{L}$ and lying in the (111) plane. For a crystal of cubic symmetry, birefringence along \mathbf{l} leads for a crystal of cubic symmetry to the following increment to $\Delta\epsilon_{ij}$:

$$\Delta\epsilon_{ij}(\mathbf{L}) = \begin{pmatrix} g_1 L_x^2 & g_2 L_x L_y & g_3 L_x L_z \\ g_2 L_x L_y & g_1 L_y^2 & g_3 L_y L_z \\ g_3 L_x L_z & g_3 L_y L_z & g_1 L_z^2 \end{pmatrix}, \quad (12)$$

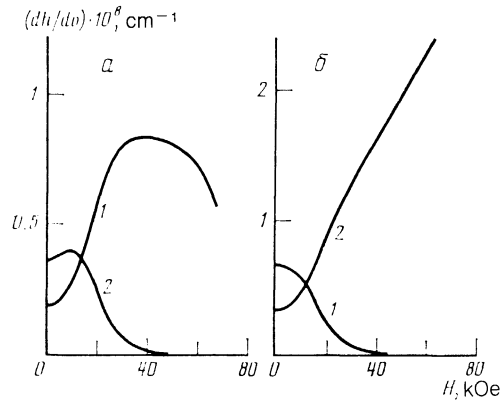


FIG. 6. Calculated field dependence of the intensity of BS by magnons of the low-frequency (a) and high-frequency (b) branches in an easy-plane AF on account of the Faraday effect: 1— $\mathbf{q} \parallel [001] \parallel \mathbf{M}$, 2— $\mathbf{q} \parallel [010] \perp \mathbf{M}$. Faraday constant $\Phi = 10^3$ rad/cm, $T = 2$ K.

where g_1, g_2 , and g_3 are the constants of the linear magnetic birefringence. In analogy with Sec. A, expansion in small deviations of \mathbf{L} yields

$$\delta\epsilon_{ij}(\mathbf{l}) = \begin{pmatrix} 0 & g_2 L_{st} l_x & 0 \\ g_2 L_{ct} l_x & 2g_1 L_{st} l_y & g_3 L_{ct} l_z \\ 0 & g_3 L_{st} l_z & 0 \end{pmatrix}. \quad (13)$$

Analysis of the dynamics of an easy-plane AF shows¹¹ that the strongest are the transverse fluctuations of \mathbf{L} in the easy plane for the lower branch of the spectrum, and only they can make a noticeable contribution of BS in EuTe. At $H = 0$, for example, the correlator $\langle l_x^2 \rangle_\Omega \propto 1/H_a$ is bounded from above only by the weak intraplanar anisotropy.

For the case $\mathbf{k}_{\text{opt}} \parallel \mathbf{q} \parallel z$, the extinction coefficient is

$$\frac{dh}{d\Omega do} = \frac{\omega^4}{32\pi^3 c^4} g_2^2 L^2 \langle l_x^2 \rangle_\Omega. \quad (14)$$

Expressing the correlator $\langle l_x^2 \rangle_\Omega$ in terms of the coordinates x', y' and z' connected with the magnetic field, and taking the fluctuation-dissipation theorem into account, we can express the right-hand side of (14) in terms of the components of the generalized-susceptibility tensor χ_{kn} of EuTe, which are given in Ref. 11:

$$\frac{dh}{d\Omega do} = \frac{\hbar \omega^4}{32\pi^3 c^4} g_2^2 (1+N(\Omega)) L^2 \{ \chi_{44} \cos^2 \varphi + \chi_{66} \sin^2 \varphi + \chi_{46} \sin 2\varphi \}, \quad (15)$$

where φ is the angle between \mathbf{H} and the (111) plane. For the particular case $\varphi = 90^\circ$ ($\mathbf{H} \parallel (111)$) we have at $kT \gg \hbar$

$$\frac{dh}{do} \propto \frac{H_E}{2H_E H_a + H^2} kT. \quad (16)$$

We see by the same token that the BS intensity at $H = 0$ is limited only by the anisotropy in the easy plane, and decreases like H^{-2} with increasing field. Figure 7 shows the calculated field dependence of the extinction coefficient for different directions of \mathbf{H} . It can be seen that the light scattering decreases strongly with increase of the projection of the magnetic field on the easy plane.

C. Exchange mechanism of one-magnon scattering of light

The expansion of the tensor $\Delta\epsilon_{ij}(\mathbf{M}, \mathbf{L})$ [see Eq. (4)] contains an isotropic term a $\delta_{ij} M^2$ that leads to a dependence

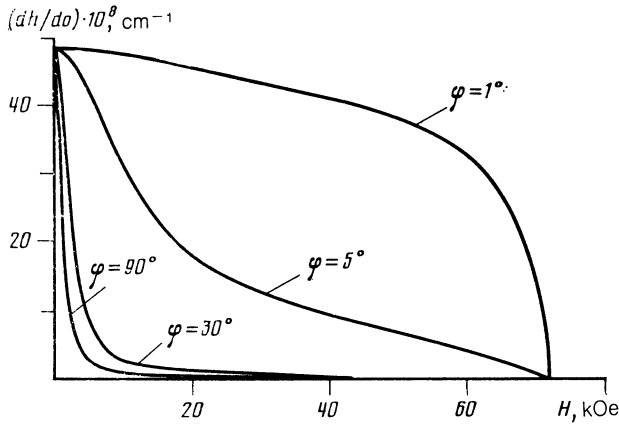


FIG. 7. Calculated field dependence of the intensity of BS by magnons of the low-frequency branch of an easy-plane AF on account of linear magnetic birefringence at various angles between H and the (111) plane, $\psi_{\text{LMB}} = 150 \text{ rad/cm}$, $T = 2 \text{ K}$.

of the refractive index on the magnetization. In this case the microscopic cause of this term is the exchange interaction between an electron in an excited d state and localized electrons in the f state (called the d - f exchange). The connection between the light wave and the spin system via the exchange interaction of the excited electron with the neighboring ions was considered earlier with an aim at explaining two-magnon scattering of light in antiferromagnets.²⁻⁴ Following these references, we demonstrate how the exchange interaction can lead not only to two-magnon but also to one-magnon scattering of light. We consider the most prevalent case, when the d - f exchange exceeds greatly the f - f exchange. In EuTe we have $J_{d-f} \sim 0.3 \text{ eV}$ and $J_{f-f} \sim 1 \text{ meV}$.

Consider two ions α and β from different magnetic sublattices, with spins S_α and S_β . Let the ion α have in the ground state and electron occupying an orbital $\varphi_{\alpha 0}(\mathbf{r}_1)$ with spin σ_α , and let the ion β have an electron on an orbital $\varphi_{\beta 0}(\mathbf{r}_2)$ with spin σ_β . We designate the orbitals of the excited states of ions α and β by $\varphi_{\alpha\mu}(\mathbf{r}_1)$ and $\varphi_{\beta\nu}(\mathbf{r}_2)$, respectively. The Hamiltonian of the interaction of the electrons with the light-wave field and with one another takes the form

$$\mathcal{H}_v = -e(\mathbf{r}_1 + \mathbf{r}_2) \cdot (\mathbf{E}_1 + \mathbf{E}_2) + e^2/r_{12}, \quad (17)$$

where \mathbf{E}_1 and \mathbf{E}_2 are the electric fields of the incident and scattered waves, and $r_{12} = |\mathbf{r}_1 - \mathbf{r}_2|$.

Inelastic scattering of light by spin waves is a perturbation-theory process of third order in the interaction \mathcal{H}_v (17). The electronic-transition scheme that illustrates the light scattering is shown in Fig. 8. After absorbing a photon of energy $\hbar\omega_1$, the electron of one of the ions (say, α) goes over into an excited state $\varphi_{\alpha\mu}$. In the excited state it experiences exchange interaction with the ground-state electrons of the neighboring ion β . The third stage constitutes an electro-dipole transition of the electron to the ground state $\varphi_{\alpha 0}$ with emission of a photon of energy $\hbar\omega_2$. As the basis wave functions used for perturbation-theory calculation of the matrix elements, we choose for the excited state wave functions such that their quantization axis σ coincides with the quantization axis of the spin in the unexcited state. The matrix element of the interaction of the light wave with the pair of ions α and β , with allowance for their exchange interaction, takes the following form (similar to Eq. (42) of Ref. 4):

$$M_{\alpha\beta} = \sum_{\mu\nu} \left\{ \frac{\langle \varphi_{\alpha 0} | e \mathbf{E}_2 \mathbf{r}_1 | \varphi_{\alpha\mu} \rangle V_{\mu} \langle \varphi_{\alpha\mu} | e \mathbf{E}_1 \mathbf{r}_1 | \varphi_{\alpha 0} \rangle}{(E_{\mu} - \hbar\omega_1)(E_{\mu} - \hbar\Omega - \hbar\omega_2)} + \left(\begin{array}{l} \mathbf{r}_1 \leftrightarrow \mathbf{r}_2 \\ \alpha \leftrightarrow \beta \\ \mu \leftrightarrow \nu \end{array} \right) S_{\alpha} S_{\beta} \right\} \quad (18)$$

$\hbar\Omega$ is the magnon energy, ω_1 and ω_2 are the frequencies of the incident and scattered waves,

$$V_{\mu 0} = \langle \varphi_{\alpha\mu}(\mathbf{r}_2) \varphi_{\beta 0}(\mathbf{r}_1) | e^2/r_{12} | \varphi_{\alpha\mu}(\mathbf{r}_1) \varphi_{\beta 0}(\mathbf{r}_2) \rangle$$

is the exchange integral between electrons in the excited state μ of the ion α and an electron localized in the ground state of the neighboring ion β (d - f exchange in the case of EuTe). Note that the electro-dipole matrix elements connect only states with different parity and like electron spin projections. To obtain the effective Hamiltonian of the interaction between an electromagnetic wave and a spin system we must sum the matrix element $M_{\alpha\beta}$ over all the pairs of ions α and

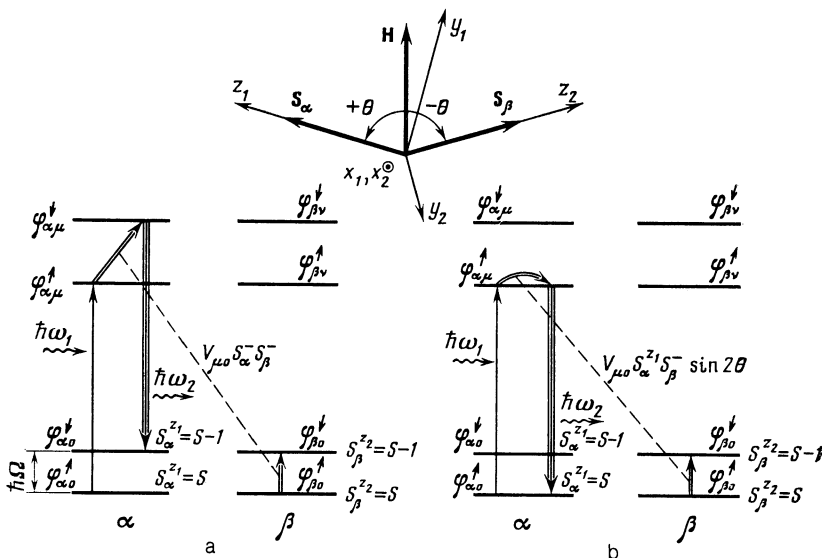


FIG. 8. Scheme of electronic transitions in the exchanges mechanism in an antiferromagnet: a—two-magnon scattering, b—one-magnon scattering.

β from each magnetic sublattice, with allowance for the required magnetic symmetry of the crystal.⁴ For a crystal of any symmetry, however, the Hamiltonian will contain a term of the form

$$\mathcal{H} = \sum_{\alpha\beta} A(\mathbf{E}_1\mathbf{E}_2) (S_\alpha S_\beta), \quad (19)$$

$$A \approx \sum_{\mu\nu} \left\{ \frac{e^2}{(E_\mu - \hbar\omega)^2} |\langle \varphi_{\alpha\mu} | \mathbf{r} | \varphi_{\alpha\nu} \rangle|^2 V_{\mu 0} + \left(\begin{matrix} \mu \leftrightarrow \nu \\ \alpha \leftrightarrow \beta \end{matrix} \right) \right\}.$$

Let the angle between the magnetic sublattices of the AF in an external magnetic field be 2θ . We express the Hamiltonian (19) in terms of the projections of the operators S_α and S_β on their proper coordinate axes x_1, y_1, z_1 and x_2, y_2, z_2 (see Fig. 8):

$$\begin{aligned} \mathcal{H} &= \sum_{\alpha\beta} A(\mathbf{E}_1\mathbf{E}_2) (S_\alpha S_\beta) \\ &= \sum_{\alpha\beta} A(\mathbf{E}_1\mathbf{E}_2) \left\{ -\frac{i}{2} \sin 2\theta [S_\alpha^{z_1} (S_\beta^+ - S_\beta^-) \right. \\ &\quad \left. - S_\beta^{z_2} (S_\alpha^+ - S_\alpha^-)] \right. \\ &\quad \left. + [\cos 2\theta S_\alpha^{z_1} S_\beta^{z_2} + \frac{1}{4} (S_\alpha^+ + S_\alpha^-) (S_\beta^+ + S_\beta^-) \right. \\ &\quad \left. - \frac{1}{4} \cos 2\theta (S_\alpha^+ - S_\alpha^-) (S_\beta^+ - S_\beta^-) \right\}. \quad (20) \end{aligned}$$

Here $S_\alpha^+, S_\alpha^-, S_\beta^+, S_\beta^-$ are operators that change by unity the projections of the spins of α and β on their proper axes z_1 and z_2 (see Fig. 8). The second term in the curly brackets of (20) describes the previously considered²⁻⁴ two-magnon scattering of light, since it causes spin flip in both sublattices. The first term in the curly brackets of (20), however, causes only one spin to overturn and therefore leads to one-magnon scattering of light even in the exchange approximation.¹² It might seem at first glance that this term is antisymmetric in the indices of the ions α and β and vanishes when summed over them. Actually, however, it is symmetric with respect to α and β , since a substitution $\alpha \leftrightarrow \beta$ must be accompanied by a substitution $\theta \leftrightarrow -\theta$. Thus, light scattering with, say, emission of magnons is described in the Hamiltonian (20) by the following terms: one-magnon scattering

$$\mathcal{H}^{(1)} = \sum_{\alpha\beta} AS \sin 2\theta (\mathbf{E}_1\mathbf{E}_2) (S_\alpha^- - S_\beta^-), \quad (20.1)$$

two-magnon scattering

$$\mathcal{H}^{(2)} = \sum_{\alpha\beta} A(1 - \cos 2\theta) (\mathbf{E}_1\mathbf{E}_2) (S_\alpha^- S_\beta^-). \quad (20.2)$$

Returning to the electronic-transition scheme (Fig. 8), we see that in a noncollinear magnetic structure, with allowance for exchange interaction, two different processes of inelastic light scattering are possible between an excited electron of one ion and unexcited electrons of the other ion. In the first, spin reversal of both the excited electron and of the electron in the ground state takes place. This changes by unity the projections of the spins on the proper quantization axes z_1 and z_2 of both ions α and β , i.e., to creation [see (20.2)] (absorption) of two magnons. If the sublattices are canted, however ($\sin 2\theta \neq 0$), the exchange interaction can alter the spin projection of only one unexcited electron belonging to the ion β , while the spin of the electron excited on

the neighboring ion α may remain unchanged. In such a process, only one ion (β) changes its spin projection [see (20.1)], and inelastic scattering of light can take place with emission (absorption) of one magnon. In a collinear system, the exchange mechanism of one-magnon scattering of light is forbidden.

Thus, in a canted magnetic structure ($\sin 2\theta \neq 0$) exchange interaction can lead not only to two-magnon but also to one-magnon inelastic scattering of light, which takes place, as seen from (20), without rotation of the light-polarization plane.

The calculation described above demonstrates only the feasibility in principle of light scattering with emission or absorption of one magnon in the pure exchange approximation. In real compounds, the scattering picture is much more complicated. Several levels can participate in electro-dipole transitions, can be split by spin-orbit interaction [as in the case of EuTe (Ref. 14)], etc. We continue the calculations using a phenomenological approach similar to subsections A and B of the present section. It can be seen from (19) that exchange interaction between an electron in an excited state and unexcited electrons leads to an isotropic term in the expansion of the dielectric tensor

$$\Delta \epsilon_{ij}(\mathbf{M}) = a \delta_{ij} M^2. \quad (21)$$

Expanding (21) in powers of the small deviation m , we get

$$\delta \epsilon_{ij} = 2a \delta_{ij} (\mathbf{M}_{st} \mathbf{m}). \quad (22)$$

Thus, the BS connected with (22) will take place if there exist in the system longitudinal oscillations of magnetization and a sufficiently large \mathbf{M}_{st} . Such a situation is realized in AF if the sublattices are strongly canted ($\theta < \pi/2$). If the AF is compensated ($H = 0, \theta = \pi/2, M = 0$), Eq. (21) contributes only to the two-magnon light scattering considered in Refs. 2-4. In an isotropic ferromagnet, the mechanism considered can lead to neither one- nor two-magnon scattering of light. The BS intensity can be obtained from (3) and (22)

$$\frac{dh}{d\Omega d\omega} = \frac{\omega^4}{32\pi^3 c^4} 4a^2 M_{st}^2 \langle m_z^2 \rangle_a \quad (23)$$

or, with allowance for the fluctuation-dissipation theorem

$$\frac{dh}{d\Omega d\omega} = \frac{\hbar\omega^4}{8\pi^3 c^4} a^2 M_{st} \text{Im}(\chi_{33}(\Omega)) (1 + N(\Omega)). \quad (24)$$

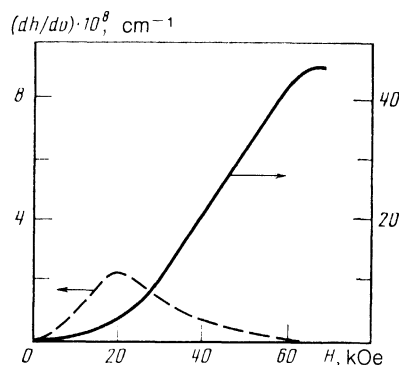


FIG. 9. Phase diagram in the (T, H) plane at $J_0 = 1.8$ (Fig. 3a) and $J_0 = 1.7$ (Fig. 3b). The inset of Fig. 3a shows in enlarged scale the phase-diagram section near the triple point. The dashed line shows the slope of the $T_N(H)$ curve in the nonergodic phase.

According to (19) and (22), the BS connected with the exchange mechanism has the following distinctive features: it is isotropic, i.e., independent of the direction of \mathbf{k}_{opt} relative to the magnetization, and takes place without rotation of the polarization plane. The exchange contribution to BS was experimentally detected by us in a study of scattering by microwave-field-excited magnons in EuTe.⁵ [Figure 9 shows the field dependence of the extinction coefficient (24) integrated over frequency, for both branches of the AF excitation spectrum of EuTe. The phenomenological constant $a = 3 \cdot 10^{-7} \text{G}^{-2}$ was taken from Ref. 5.

To conclude this section, we emphasize once more that the mechanism considered, based on d - f exchange interaction (it is usually of the order of 0.1–1 eV) leads to one-magnon scattering of light in canted magnetic structure even if spin-orbit interaction is absent or is ineffective.

7. FIELD DEPENDENCE OF BRILLOUIN SCATTERING INTENSITY IN EuTe. COMPARISON OF THEORY WITH EXPERIMENT

As noted above, we have measured the intensity of BS by magnons of the low-frequency branch of the spectrum as a function of the applied magnetic field (see Fig. 5). Comparison of the experimental results with calculation has shown that the best agreement is obtained if account is taken of the BS contributions from all three MOE described in Sec. 6.

In weak fields, BS by magnons of the low-frequency branch is mainly due to LMB. Notwithstanding the relative weakness of LM in EuTe ($\psi_{\text{LMB}} = 150 \text{ rad/cm}$), the anomalously large fluctuations of the vector \mathbf{L} in the easy plane lead to an appreciable intensity of the BS in weak fields (see Fig. 7). With increase of the projection of the magnetic field on the easy plane, the extinction coefficient decreases like $1/H^2$ and the LMB ceases to make a noticeable contribution to the scattering even in fields 5–7 kOe.

The FE makes a rather small contribution to scattering by magnons of the low-frequency branch. In BS by magnons of the high-frequency branch, however, it does play a decisive role. The fact that scattering by such magnons was recorded also in weak fields can be explained only when account is taken of the FE (see Fig. 6). Moreover, the intensity of BS by high-frequency magnons in strong fields ($H \gtrsim H_E$) depended strongly on the direction of \mathbf{k}_{opt} . No BS could be recorded in fields $H > 40 \text{ kOe}$ at $\mathbf{k}_{\text{opt}} \parallel \mathbf{H}$, whereas at $\mathbf{k}_{\text{opt}} \perp \mathbf{H}$ the scattering intensity was relatively large and showed no tendency to decrease with increase of H . All this is also in agreement with the calculation results (Fig. 6).

In fields stronger than 20 kOe, the main contribution to BS by low-frequency magnons is made by IMR due to d - f exchange interaction. As already noted, the intensity of the

scattering due to IMR is isotropic, i.e., is independent of the direction of \mathbf{k}_{opt} , as is indeed observed in experiment.

The solid curves of Fig. 5 show the calculated contributions of each of the described MOE to the BS intensity and the total scattering intensity. The curves were plotted using the numerical values of the constants of the Faraday-effect and of the isotropic magnetic refraction from Ref. 5, and the normalization to the ordinate axis was chosen to obtain best agreement between the experimental data and the calculated curves. It can be seen that it was possible not only to separate the contribution of each MOE, but also to obtain good quantitative agreement between theory and experiment.

The authors are sincerely grateful to A. S. Borovik-Romanov for valuable advice and remarks, V. M. Loktev and A. V. Chubukov for helpful discussions, and L. Minkova (Institute of Solid State Physics, USSR Academy of Sciences), for kindly supplying the EuTe crystals.

¹¹It can be due both to crystallographic anisotropy and to hyperfine or magnetoelastic interactions.

¹²It is known that in an antiferromagnetic transition the rhombohedral distortion of the crystallographic lattice of EuTe are small.

¹A. S. Borovik-Romanov and N. M. Kreines. Phys. Rept. **81**, 5 (1982).

²V. S. L'vov, Zh. Eksp. Teor. Fiz. **53**, 163 (1967) [Sov. Phys. JETP **26**, 113 (1968)].

³T. J. Moriya, J. Phys. Soc. Jpn. **23**, 190 (1967).

⁴P. A. Fleury and R. Loudon, Phys. Rev. **166**, 514 (1968).

⁵S. O. Demokritov, N. M. Kreines, and V. I. Kudinov, Pis'ma Zh. Eksp. Teor. Fiz. **41**, 38 (1985) [JETP Lett. **41**, 46 (1985)].

⁶W. R. Johnson and P. C. McColum, Phys. Rev. **B22**, 2435 (1980).

⁷G. Will, S. J. Pickort, H. A. Alperin, and R. J. Nathans, Phys. Chem. Sol. **24**, 1679 (1963).

⁸W. Battles and G. E. Everett, Phys. Rev. **B1**, 3021 (1970).

⁹N. F. Oliveira, S. Foner, J. Shapira, and T. B. Reed, Phys. Rev. **B21**, 169 (1980).

¹⁰P. K. Strelt and G. E. Everett, Phys. Rev. **B21**, 169 (1980).

¹¹A. S. Borovik-Romanov, S. O. Demokritov, N. M. Kreines, and V. I. Kudinov, Zh. Eksp. Teor. Fiz. **88**, 1348 (1985) [Sov. Phys. JETP **61**, (1985)].

¹²S. O. Demokritov, N. M. Kreines, and V. I. Kudinov, Pis'ma Zh. Eksp. Teor. Fiz. **45**, 312 (1986) [sic].

¹³J. Schoenes and P. Wachter, Physica (Utrecht), **86–88**, 125 (1977).

¹⁴G. Guntherodt, P. Wachter, and D. M. Imboden, Phys. Kond. Mat. **12**, 282 (1971).

¹⁵J. Feinleib and C. R. Pidgeon, Phys. Rev. Lett. **23**, N24, 1391 (1969).

¹⁶V. V. Lemanov and G. A. Smolenskii, Usp. Fiz. Nauk **108**, 465 (1972) [Sov. Phys. Usp. **15**, 708 (1973)].

¹⁷A. I. Akhiezer, V. G. Bar'yakhtar, and S. V. Peletminskii, Spin Waves, Nauka, 1967.

¹⁸I. A. Akhiezer and Yu. L. Bolol'tin, Zh. Eksp. Teor. Fiz. **53**, 267 (1967) [Sov. Phys. JETP **26**, 179 (1968)]; Fiz. Tverd. Tela (Leningrad) **9**, 2559 (1967) [Sov. Phys. Solid State **9**, 2008 (1967)].

¹⁹L. D. Landau and E. M. Lifshitz, *Electrodynamics of Continuous Media*, Pergamon, 1984.

²⁰L. D. Landau and E. M. Lifshitz, *Statistical Physics*, Part 1, Pergamon

Translated by J. G. Adashko